

Enhanced CO Tolerance for Hydrogen Activation in Au–Pt Dendritic Heteroaggregate Nanostructures

Shenghu Zhou, Kevin McIlwrath, Greg Jackson, and Bryan Eichhorn*

Departments of Chemistry and Biochemistry, and Mechanical Engineering, University of Maryland, College Park, Maryland 20742, and Hitachi Instruments, Hitachi High Technologies America, 5100 Franklin Drive, Pleasanton, California 94588

Received October 10, 2005; E-mail: eichhorn@umd.edu

We report here the synthesis, characterization, and unusual catalytic properties of Au–Pt dendritic heteroaggregate nanostructures for oxidation reactions in CO/H₂ mixtures. PtAu bimetallic nanoparticles (NPs) have been extensively studied for a variety of catalytic applications. PtAu bimetallics as well as Au@Pt and Pt@Au core–shell NPs have all been prepared and characterized.^{1–4} Reactivity studies show that the catalytic behavior in this bimetallic system is dependent upon the NP architecture and is significantly different from that of the individual metal NPs. In particular, a recent study of the AuPt bimetallic NPs prepared through dendrimer-based synthesis showed that CO oxidation was greatly enhanced relative to the pure Pt and Au NP systems.²

The use of CO-contaminated H₂ fuels in low-temperature fuel cells will be facilitated by anode catalysts that oxidize CO while maintaining high activity for H₂ electrooxidation at temperatures under 100 °C. While CO oxidation can be significantly enhanced in various monometallic^{5–8} and bimetallic nanostructures,² these systems have often been designed strictly for preferential oxidation of CO at low temperatures with reduced activity for H₂ oxidation. For example, supported Au-based nanocatalysts show remarkable CO oxidation behavior at very low temperatures,^{5–8} but their ineffectiveness as H₂ oxidation electrocatalysts does not make them attractive candidates for fuel cell anode applications. In contrast, excellent H₂ activators, such as Pt NPs, are poisoned by CO below 100 °C. While some alloy NPs, such as the PtRu systems,⁹ have shown promise as CO-tolerant H₂ electrocatalysts, the presence of CO above a few 100 ppm still causes a significant drop in the H₂ oxidation kinetic rates below 100 °C. The lack of a mechanistic understanding of the Pt–Ru system limits the ability for developers to optimize this system. With their very high selectivity for CO oxidation and high H₂ thermal oxidation activity below 100 °C in mixed CO/H₂ fuel streams, the Au–Pt dendritic heteroaggregate nanostructures reported here show potential to overcome these limitations. Comparing this system to Pt–Ru systems suggests that the Pt–Au NPs may be an excellent candidate for a low-temperature anode electrocatalyst.

Monometallic Pt (5 nm) and Au (11 nm) NPs were prepared by employing minor modifications of published procedures.¹⁰ The Au–Pt heteroaggregate particles were prepared using modified standard procedures for sequential core–shell particle growth. The Au core was prepared by reducing HAuCl₄ in a decahydronaphthalene/oleylamine mixture (~6:1, v:v) at 110 °C for 12 h. The resulting purple colloidal solution was cooled to room temperature, charged with Pt(acac)₂ (1:1, Pt:Au), and refluxed for an additional 2 h. The Pt–Au particles were precipitated from the resulting dark colloidal mixture (ethanol and centrifugation), washed (acetone), and re-suspended in toluene. All supported catalysts were prepared by adding γ -alumina (80–120 m² g⁻¹, 3 μ m) to the corresponding colloidal toluene suspensions and subsequently removing the toluene

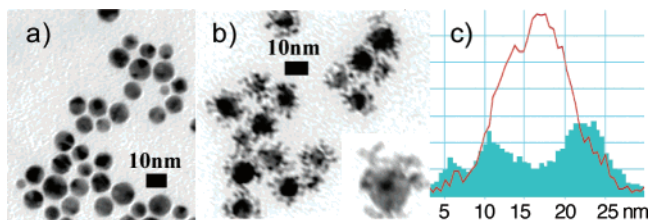


Figure 1. TEM images of (a) Au NP core particles, (b) Au–Pt dendritic aggregates (particle enlargement in inset), and (c) EELS line scan across the Au–Pt particle showing atomic composition (Au-red, Pt-green) as a function of beam displacement across the particle. Particle center occurs at ~18 nm.

solvent in vacuo. All catalyst loadings were prepared to contain 1.0 wt % Pt. The Au control catalyst was 1.0 wt % Au.

The Au–Pt heteroaggregate NPs have been characterized by XRD, EDX, TEM, STEM phase mapping, and EELS single particle analysis. The TEM images (Figure 1 and S-1) show that the Au NP precursor and the Au cores of the heteroaggregate structures are identical in size (6–18 nm range; 11 nm, av.). The TEM image of the bimetallic (Figure 1b) shows that the Pt metal grows from the Au seed as dendritic tendrils (~7 nm diameter) to form a heteroaggregate structure that is architecturally distinct from the bimetallic and core–shell AuPt systems previously reported.^{1–4} The heteroaggregate structure is consistent with the XRD patterns of the “as prepared” NPs, which show non-alloyed Au peaks with shoulders arising from the Pt tendrils. Annealing the sample at 400 °C for 3 h crystallizes the Pt components to give well-defined Pt and Au diffraction patterns (Figure S-2). STEM phase mapping (Figure S-3) is also consistent with dendritic Pt tendrils extending from the Au core, but the overlap in the X-ray lines complicates the interpretation. Definitive evidence of the Au core/Pt tendrill structure is seen in the EELS line scans across individual heteroaggregate particles (Figures 1c and S-3). The data show that the core is essentially pure Au, whereas the Pt density is concentrated at the periphery of the particles. EDX analysis of the bulk sample is consistent with a 1:1 mixture of Pt and Au. The data give a consistent picture of a pure Au core with Pt tendrils attached to the Au particle surface. This unique dendritic heterostructure is similar to the dendritic manganese oxide nanostructures¹¹ and related nano-multipods,¹² except that the bimetallic heterostructure described here has a core that is compositionally distinct from the tendrils. This behavior contrasts typical core–shell seeded growth mechanisms but is consistent with the PtAu phase diagram and related heterodimer particle syntheses.¹³ The aggregate structure and the lack of any monometallic particles in the colloidal suspension strongly suggests that Pt growth is templated on the Au surface. The dendritic heteroaggregate structure of the current Au–Pt system gives rise to anomalous catalytic properties not observed in any of the other monometallic or bimetallic architectures.

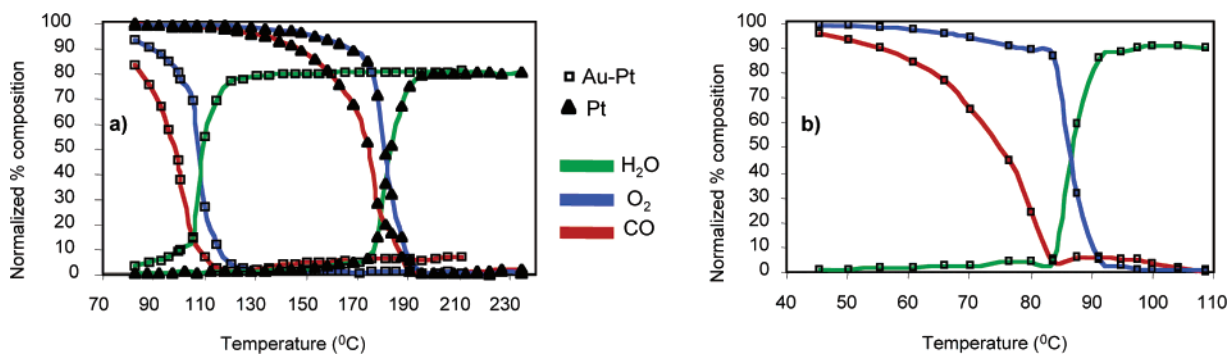


Figure 2. Temperature-programmed oxidation reactions. (a) Comparison of Pt and Au–Pt heteroaggregate catalysts for H₂ oxidation in H₂/CO/O₂ fuel streams (50:0.2:0.5) with Ar balance. CO and O₂ are normalized to inlet composition. H₂O composition is normalized with respect to H₂O generated if the limiting reactant O₂ were completely converted to H₂O. When all O₂ and CO are consumed, 80% of the O₂ is used to form H₂O and the other 20% is used for conversion of CO to CO₂. (b) H₂ oxidation with the Au–Pt heteroaggregate catalyst in 1000 ppm CO (H₂/CO/O₂ fuel streams, 50:0.1:0.5) showing the 84 °C H₂ lightoff. The 90% maximum for normalized H₂O composition is again based on O₂, and the remaining 10% is used for CO oxidation.

Temperature-programmed reactor experiments (TPR) for oxidation of CO-contaminated H₂ fuels were conducted to estimate the potential of the Au–Pt heteroaggregates for CO-tolerant H₂ electrooxidation catalysts. The alumina-supported catalysts were exposed to streams of H₂/CO/O₂ flowing at 21 cm/s, and the exhaust was continuously monitored by mass spectrometry (Thermo Prima δB). Oxygen-deficient fuel streams were employed to evaluate the discrimination between CO versus H₂ oxidation. The initial experiments were conducted with 2000 ppm CO concentrations and a hydrogen-to-CO ratio of 250:1. The results (Figure 2a) show that the activity of the monometallic Pt catalyst is significantly impeded by the CO impurity, which raises the H₂ lightoff temperature to 175 °C. In pure H₂, the same Pt catalyst has a 50 °C lightoff and achieves 100% O₂ conversion by 60 °C. In contrast, the Au–Pt heteroaggregate catalyst is significantly more active in the presence of CO, showing a 105 °C lightoff under identical conditions and Pt loadings. Note that less than 1% of the H₂ is consumed and the observed 80% yield of water is based on the limiting reagent, O₂. The remaining 20% of the O₂ is used for the oxidation of CO to CO₂. Control experiments were also conducted in which Au NPs and monometallic Au/Pt NP mixtures were co-deposited from colloidal suspensions and evaluated under the same conditions and loadings (Figure S-4). The Au catalysts had little activity for CO or H₂ oxidation under 200 °C. It is well-known^{5–8} that Au NPs larger than 5 nm are not active for CO oxidation, and the lack of reactivity from the 11 nm NPs described here is not surprising. Moreover, the monometallic Au/Pt mixture displayed reactivity very similar to that of pure Pt (Figure S-4). The remarkable enhancement in CO tolerance observed for the Au–Pt heteroaggregate catalyst is due to its bimetallic nature and its heteroaggregate architecture and is not just a function of its elemental composition.

To further probe the relationship between CO contamination and H₂ lightoff, we evaluated the AuPt heteroaggregate catalyst for H₂ oxidation in a 1000 ppm CO fuel stream. The results (Figure 2b) show that H₂ lightoff drops to 84 °C and 100% oxygen conversion by 92 °C. Again, the observed 90% yield of water is based on O₂ feed concentrations, and less than 1% of the H₂ is consumed. Additional tests in highly O₂-deficient feeds (H₂/CO/O₂ = 50:0.45:0.2) show that CO is selectively oxidized (see Figure S-4).

In the Pt and Au–Pt heteroaggregate TPR experiments, CO oxidation and H₂ lightoff are clearly linked. CO oxidation precedes

H₂ lightoff in both experiments and reaches completion in the 1000 ppm CO case. This observation is consistent with CO poisoning models in which strong CO binding to Pt surfaces blocks sites for O₂ and H₂ activation. Since CO does not bind strongly to large Au NPs, we speculate that the Au core most likely activates O₂ and facilitates¹⁴ CO oxidation at the Au–Pt interface (the triple-phase boundary). By oxidizing the CO at the interface, the Pt tendrils are cleansed of CO contaminants and resume their primary function as H₂ oxidation catalysts. The detailed mechanism for enhanced CO tolerance of the Au–Pt heteroaggregate NPs is currently under investigation in order to explore the potential use of these catalyst for CO-tolerant anodes in low-temperature fuel cell applications.

Acknowledgment. This material is based upon work supported by the National Science Foundation under Grant No. 0401850, and the U.S. Department of Energy’s Oak Ridge National Lab under the Advanced Reciprocating Engine Systems Program. We thank Dr. Ray Tweston of Gatan for assistance with the EELS data.

Supporting Information Available: Additional TEM data, particle phase maps, EELS data, control reactivity studies, and experimental details (5 pages, print/PDF). This material is available free of charge via the Internet at <http://pubs.acs.org>.

References

- (1) Zhang, B.; Li, J. F.; Zhong, Q. L.; Ren, B.; Tian, Z. Q.; Zou, S. Z. *Langmuir* **2005**, *21*, 7449–7455.
- (2) Lang, H.; Maldonado, S.; Stevenson, K. J.; Chandler, B. D. *J. Am. Chem. Soc.* **2004**, *126*, 12949–12956.
- (3) Wu, M. L.; Chen, D. H.; Huang, T. C. *Chem. Mater.* **2001**, *13*, 599–606.
- (4) Henglein, A. *J. Phys. Chem. B* **2000**, *104*, 2201–2203.
- (5) Bulushev, D. A.; Yuranov, I.; Suvorova, E. I.; Buffat, P. A.; Kiwi-Minsker, L. *J. Catal.* **2004**, *224*, 8–17.
- (6) Daniells, S. T.; Overweg, A. R.; Makkee, M.; Moulijn, J. A. *J. Catal.* **2005**, *230*, 52–65.
- (7) Kung, H. H.; Kung, M. C.; Costello, C. K. *J. Catal.* **2003**, *216*, 425–432.
- (8) Chen, M. S.; Goodman, D. W. *Science* **2004**, *306*, 252–255.
- (9) Avgouropoulos, G.; Ioannides, T. *Appl. Catal. B* **2005**, *56*, 77–86.
- (10) Hiramatsu, H.; Osterloh, F. E. *Chem. Mater.* **2004**, *16*, 2509–2511.
- (11) Yuan, J.; Li, W. N.; Gomez, S.; Suib, S. *J. Am. Chem. Soc.* **2005**, *127*, 14184–14185.
- (12) Zitoun, D.; Pinna, N.; Frolet, N.; Belin, C. *J. Am. Chem. Soc.* **2005**, *127*, 15034–15035.
- (13) Gu, H.; Yang, Z.; Gao, J.; Chang, C. K.; Xu, B. *J. Am. Chem. Soc.* **2005**, *127*, 34–35.
- (14) Deng, X.; Min, B. K.; Guloy, A.; Friend, C. M. *J. Am. Chem. Soc.* **2005**, *127*, 9267–9270.

JA056924+